

Design study of a capacitive pressure sensor in non-silicon materials

M.H.H. Meuwissen, E.P. Veninga, M.W.W.J. Tjndink, M.G.H. Meijerink

TNO Science and Industry, P.O. Box 6235, NL 5600 HE Eindhoven, The Netherlands
Telephone +31 40 26 50 482 Fax +31 40 26 50 305 E-mail marcel.meuwissen@tno.nl

Abstract

This paper reports on the design of a capacitive pressure sensor fabricated in non-silicon materials. The sensor consists of a thin membrane placed parallel to a rigid reference plane. The membrane and the reference plane act as the two electrodes of a capacitor. Deflection of the membrane due to a pressure difference results in a change in capacity. These capacity changes are processed to calculate the pressure on the membrane.

The sensor is mounted on a Low Temperature Co-fired Ceramic (LTCC) substrate. Compared to standard ceramic substrate materials, LTCC allows for the integration of interconnect, actives and passives inside the substrate thereby creating a compact way of packaging and interconnecting electronic components. Moreover, LTCC exhibits excellent dielectric properties, has good hermiticity, and it is bio-compatible.

Several thermo-mechanical performance aspects of the sensor are addressed during the design stage. Promising variants of the sensor are built and subjected to (thermo-) mechanical tests. In addition, use is made of numerical techniques to assess the performance of certain variants in an early stage.

The application of this combination of physical experiments and numerical simulations is demonstrated for the selection of a suitable membrane material and membrane dimensions (in terms of induced stresses and lateral deflection during operation). In addition, this design approach is utilised for the selection of a suitable solder interconnect material and interconnect dimensions. A critical aspect in the latter case was the creep behaviour of the solder material, which had to be minimised in order to obtain sufficient long term accuracy of the sensor.

A sensor membrane and interconnect design was finally selected based on the outcome of the design studies. It proved to meet the functional demands imposed by the targeted application on a laboratory scale. It will be subjected to reliability and lifetime assessment tests in a next phase.

Keywords: pressure sensor, assembly and packaging, soldering, AuSn20, virtual prototyping

1. Introduction

Micromachined pressure sensors are already commercially available for many years [1,2]. They are typically fabricated in silicon which warrants their use only for applications in which they can be manufactured in large volumes because of the high costs for production facilities. In order to enable the production of low- and mid-volume series at reasonable unit prices, the materials and production costs have to be reduced considerably. This could possibly be achieved by the use of other materials and processes that are commonly applied in micro-electronics.

The principle of the current pressure sensor is schematically shown in Fig. 1.

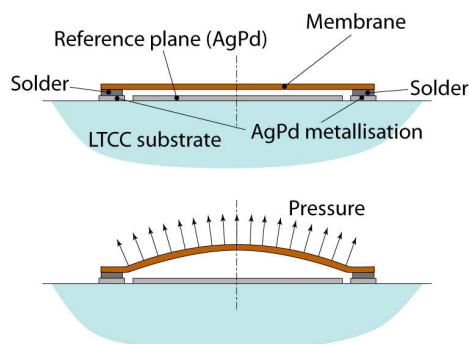


Fig. 1. Pressure sensor consisting of a thin circular membrane mounted onto a Low-Temperature Co-fired Ceramic (LTCC) substrate.

The sensor basically consists of a thin circular membrane placed parallel to a rigid reference plane. The membrane and the reference plane act as the two electrodes of a capacitor. Deflection of the membrane due to a pressure difference results in a change in capacity. These capacity changes are logged and are used to calculate the pressure on the membrane.

2. Fabrication of pressure sensor

The sensor concept is based on a LTCC substrate (DuPont 951 material) with thick film patterns of Ag-Pd on the outer layer.

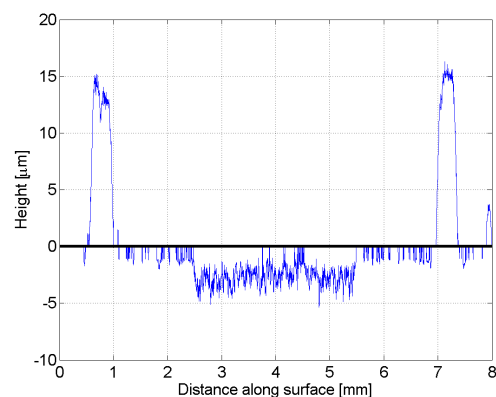


Fig. 2. Example of an laser profile meter scan over the LTCC sensor pattern. The two large peaks represent the interconnection ring, the lower section in the centre represents the middle electrode of the sensor (both Ag-Pd thick film).

Together with Via Electronic GmbH, design and fabrication parameters (printing, lamination and firing) are optimized in order to obtain flat substrates with accurate and reproducible thick film patterns.

Initially sensor variants with bare copper, Au-Ni plated stainless steel and LTCC (Ag-Pd) membranes are assembled using SnPb37 or SnAg3Cu0.5 solder as interconnection material. The later one is investigated as a lead-free variant and is expected to exhibit a higher resistance to creep [3]. The solders are either applied by screen printing solder paste or by placing solder performs in combination with a gel flux (ANSI / J-STD-004: ROL0). A flip chip bonder is used to align the membranes and to maintain an off-set in z-direction during soldering.

3. Membrane material and dimensions selection

For selecting a suitable membrane material and dimensions (diameter and thickness), a numerical model is used to calculate the response of the membrane to pressure loads. Because of the simple shape of the sensor membrane, a fairly straightforward analytical model can be applied. A change in pressure is detected electrically by a change in capacity. The capacity C for the current configuration is determined from:

$$C(p) = \int_{r=0}^{R_e} \frac{2\pi\epsilon}{h(r,p)} dr, \quad (1)$$

where R_e is the radius of the rigid reference plane, ϵ is the dielectric constant of the medium between the two electrodes, p is the pressure on the membrane and h is the distance between the upper and the lower electrode (see Fig. 3).

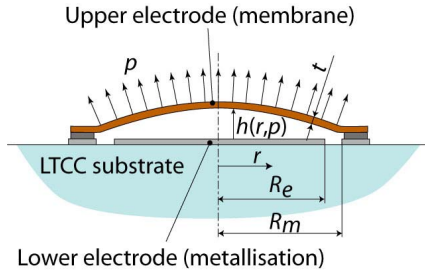


Fig. 3. Explanation of symbols.

The distance between the lower electrode and the membrane is the sum of the initial distance at zero pressure (h_0) and the deflection of the membrane due to the applied pressure. For a clamped circular plate loaded by a uniform pressure, the deflection w is given by [4]:

$$w(r) = \frac{p(R_m^2 - r^2)^2}{64D}, \quad (2)$$

with R_m the radius of the membrane and D the flexural rigidity:

$$D = \frac{Et^3}{12(1-\nu^2)}, \quad (3)$$

where E is the Young's modulus, ν is the Poisson's ratio, and t is the plate thickness.

Using Eqs. (1) to (3), the membrane deflection and capacity changes can be calculated for different configurations. The results are summarized in Table 1.

Table 1. Maximal deflection and capacity change due to an applied pressure of 5 bar for several configurations. Initial gap distance h_0 is 40 μm and lower electrode radius R_e is 1.5 mm for all configurations.

Configuration		Capacity change [pF]	Maximal deflection of centre [μm]
Material	t [μm]		
Cu	200	0.10	3.5
Cu	100	1.57	27.7
Fe-Cr-x	100	0.64	16.6
LTCC	270	0.05	1.7
LTCC	270	0.24	6.5
LTCC	135	0.48	13.6
Kovar	250	0.04	1.5

The lowest sensitivity is calculated for the Kovar membrane. In addition, the thick copper membrane (200 μm) and the thick LTCC membrane (270 μm) with the same diameter have a relatively low sensitivity as well. The other configurations have significantly higher sensitivities.

4. Measured response of the membrane

Fig. 4 shows the results of an actual experiment using an LTCC membrane. In this experiment an LTCC membrane (thickness 270 μm , radius 2.5 mm) is subjected to a constant pressure for nearly 3 days. The sensor membrane is attached to the substrate by an SnAg3Cu0.5 solder alloy. The electrical capacity is measured with a 0.001 pF resolution.

For the unloaded membrane, the capacity is approximately 2.015 pF. From Eq. (1), the initial electrode distance h_0 is estimated at 31 μm . Using this estimate, the calculated capacity at 5 bar pressure is 2.09 pF, whereas the measured value is slightly less than 2.06 pF.

The sensor shows some capacity drift over the 3 day period (approximately 0.005 pF). This drift may possibly be attributed to time dependent behaviour of the solder material. After removal of the pressure, the membrane does not fully recover to its original deflection. This also indicates the presence of one or more irreversible mechanisms.

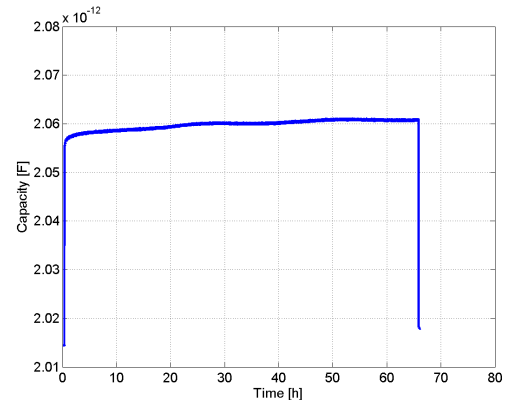


Fig. 4. Measured capacity of a 270 μm thick LTCC membrane (radius $R_m=2.5$ mm) during testing. At $t=0$ hours, 5 bar pressure is applied, held constant for nearly 66 hours and removed again.

5. Prediction of creep in solder interconnect

In order to gain some insight into the origins of the observed drift in the response of the sensor, an axi-

symmetric model is implemented in a finite element package. This model comprises of the sensor membrane and a ring of solder material placed at the periphery of the membrane. Characteristics of the mesh of this model are shown in Fig. 5. The width of the solder ring is 400 μm and its height is 40 μm . The outer radius of the membrane is 2.9 mm.

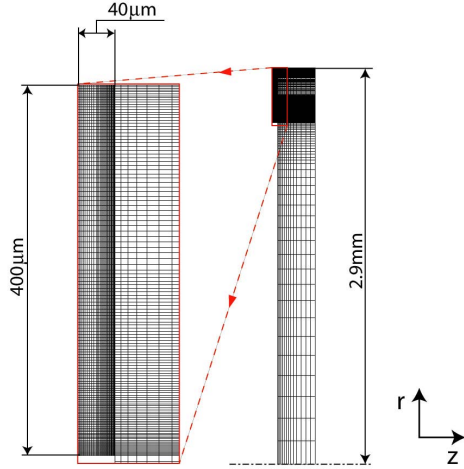


Fig. 5. Finite element mesh used for the axi-symmetric model consisting of the sensor membrane and a solder ring.

The membrane is assumed to behave linear elastically whereas a creep law is adopted for the solder material. Simulations are carried out for both SnAgCu solder and eutectic SnPb solder. For the SnAgCu solder, the following creep law is used:

$$\frac{d\varepsilon_{cr}}{dt} = C_1 [\sinh(C_2 \sigma)]^n \exp\left(\frac{E_{act}}{RT}\right) \quad (4)$$

where R is the universal gas constant, ε_{cr} the creep strain, σ the stress, and T the temperature. The parameters in Eq. (4) are taken from literature [3] and summarised in Table 2.

Table 2. Parameters used in the creep equation (4) applied for the SnAgCu solder alloy.

Parameter	Value
C_1	$7.925 \cdot 10^{-5}$
C_2	0.0356 MPa^{-1}
E_{act}	$6.7910 \cdot 10^{-4} \text{ J/mol}$
N	6

For describing the creep behaviour of the eutectic SnPb solder the following creep law is applied [5]:

$$\frac{d\varepsilon_{cr}}{dt} = C \frac{G}{T} \left[\sinh\left(\alpha \frac{\sigma}{G}\right) \right]^n \exp\left(\frac{-Q}{kT}\right), \quad (5)$$

where G is the shear modulus and k is Boltzmann's constant. The other parameters are taken from literature [6] and summarised in Table 3.

Table 3. Parameters in the creep equation (5) applied for the eutectic SnPb solder.

Parameter	Value
C	$16.534 \text{ Kmm}^2/\text{Ns}$
A	751
Q	$8.78 \cdot 10^{-20} \text{ J}$
N	3.3

The plastic behaviour of the solder material is

neglected in the current simulations. The other parameters required for the model are summarised in Table 4.

Table 4. Parameters used for the elastic part of the models.

Material	Young's modulus [GPa]	Poisson's ratio [-]
Solder (SnAgCu)	38	0.40
Solder (SnPb)	30	0.37
LTCC (membrane)	100	0.30

Fig. 6 shows the lateral deflection of the center of the membrane as a function of time for the two solder alloys. For the SnAgCu solder, the deflection increases by 0.11 μm over 3 days due to creep. From the experiments, the drift was estimated at 0.1 μm . Given the relatively large scatter on LTCC substrate thickness, the unknown thickness h_0 , and the relatively crude approximation of the creep behaviour (only second level creep included), the numerical value compares well to the experimental one. For the eutectic SnPb solder alloy, the creep over the 3 day period is much higher: about 0.88 μm .

The calculated stresses in the solder material remained well below the yield stress, indicating that the inclusion of plastic behaviour in the model for the solder is unnecessary.

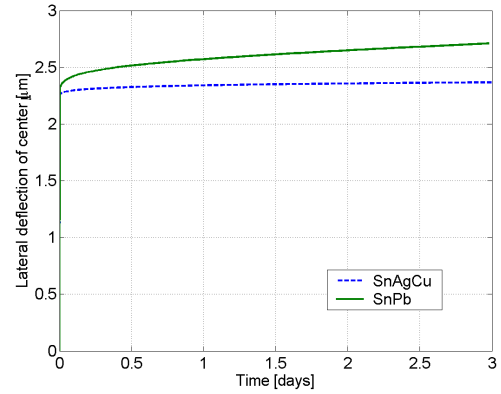


Fig. 6. Deflection of the centre of the membrane during application of a uniform pressure (5 bar).

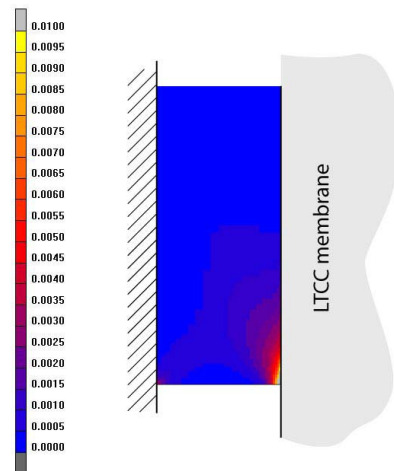


Fig. 7. Accumulated creep strain in the SnAgCu solder interconnect after 3 days under a constant pressure load of 5 bar on the membrane surface.

Fig. 7 shows a part of the SnAgCu solder material

in the region where the accumulated equivalent creep strain attains the highest values after 3 days. It can be seen that the maximal creep strain is concentrated in a corner-point (singular point). The peak values should thus be treated with care since they are mesh dependent. The strains somewhat further away are approximately 1%.

From the experimental and numerical investigations, it can be concluded that drift leads to an unacceptable disturbance of the pressure measurements. After 3 days, the drift on the lateral displacement of the membrane is already 5% for the SnAgCu material whereas a drift of less than 1% is acceptable for the current application. The simulations support the hypothesis that the drift is caused by creep in the solder interconnect.

6. AuSn solder interconnect

In order to improve the long term stability of the sensor response, the replacement of the current solder material by a more creep resistant material is considered. The AuSn20 solder alloy is known to have good creep properties. Unfortunately, the creep behaviour of this material is not as thoroughly investigated as that for the more commonly used SnPb37 and SnAgCu alloys. Due to the lack of appropriate creep models for this material, it was not possible to assess its performance by numerical simulations and therefore physical prototypes incorporating this solder material were built and tested.

By changing to AuSn20 solder, also the membrane material has to be changed. Due to the higher solidus temperature of AuSn20 ($T_{EUT} = 278\text{ }^{\circ}\text{C}$), higher stresses are induced during cooling down in case of a CTE mismatch between the substrate and the membrane. For the LTCC / stainless steel configuration ($\varnothing 5.8\text{ mm}$) this frequently resulted in a slightly warped membrane. In order to overcome this problem a Kovar (FeNiCo) membrane with a CTE of $5.5\text{ ppm}/^{\circ}\text{C}$ is selected ($\text{CTE}_{LTCC} \approx 6\text{ ppm}/^{\circ}\text{C}$). To improve the solderability of the Kovar membranes a Ni barrier and Au wetting layer is applied.

Soldering with AuSn20 on Ag-Pd is not a common practice. The first experiments showed poor wetting with de-wetting areas and excessive voiding at the interface. Acceptable results are obtained by changing from a flux with a low activity (L0) to a flux with a moderate activity (M0) and by keeping the time above the liquidus temperature during the soldering operation as short as 5 s. In addition to this, also the amount of flux needs to be controlled carefully due to an increase of the void-rate at higher flux amounts.

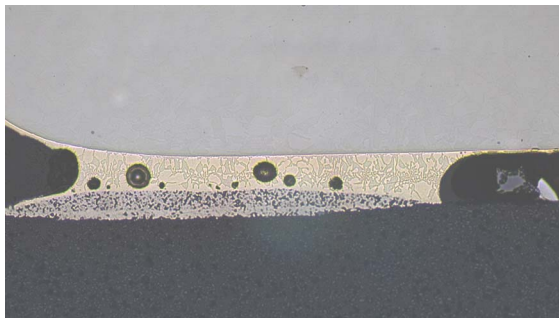


Fig. 8. Cross section of AuSn20 solder interconnection between Ni-Au plated Kovar membrane and Ag-Pd thick film on LTCC substrate.

The stability of the AuSn20 interconnection has proven

to be better than 6% full scale when exposed to 5 bar (the maximum pressure) over a period of 2 weeks. The sensitivity obtained from experimental results and an analytical analysis are shown in Fig. 9.

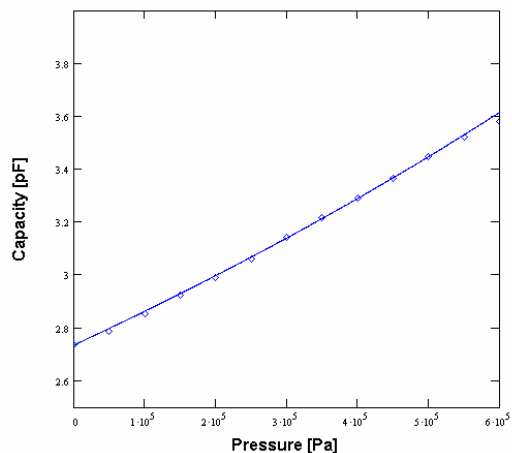


Fig. 9. Sensitivity of a pressure sensor with a stainless steel membrane ($\varnothing 5\text{ mm}$) and AuSn20 solder interconnection (diamonds: experimental data, line: numerical analysis).

7. Conclusions and future work

The initial development of a pressure sensor has been described. Based on a combination of experiments and simulations a sensor has been designed that fulfills the required demands during laboratory tests.

The study has resulted in a LTCC / Kovar configuration with a high melting temperature AuSn20 solder interconnection. In applications this configuration allows reflow soldering of additional components without re-melting the sensor interconnection.

Future work includes the testing of prototypes during operation both on their long term stability and their (thermo-mechanical) reliability.

Acknowledgements

The authors would like to thank Via Electronic GmbH for assistance during the design phase and fabricating test substrates.

References

- [1] Sze, S.M., Semiconductor sensors, John Wiley & Sons Inc. (1994).
- [2] Campbell, S.A., Lewerenz, H.J., Semiconductor machining, fundamentals & technology (1998).
- [3] Clech, J.P., Review and Analysis of Lead-Free Solder Material Properties, <http://www.metallurgy.nist.gov/solder/clech>, 2004.
- [4] Timoshenko, S.P., Woinowski-Krieger, S., Theory of plates and shells, McGraw-Hill (1959).
- [5] Darveaux, R., Banerji, K., Constitutive relations for tin based solder joints, IEEE Transactions on Components, Hybrids and Manufacturing Technology, Vol. 15, No.6 (1992) 1013–1024.
- [6] Lau, J.H., Ball Grid Array Technology, McGraw-Hill Inc., New York, 1995, Ch. 13.